



Study of the esterification reaction of acetic acid with *n*-butanol over supported WO₃ catalysts

Gheorghiță Mitran ^a, Tatiana Yuzhakova ^b, Ionel Popescu ^c, Ioan-Cezar Marcu ^{a,c,*}

^a Laboratory of Chemical Technology and Catalysis, Department of Organic Chemistry, Biochemistry & Catalysis, Faculty of Chemistry, University of Bucharest, 4-12, Blv. Regina Elisabeta, 030018 Bucharest, Romania

^b Institute of Environmental Engineering, Faculty of Engineering, University of Pannonia, 10 Egyetem St, 8200 Veszprém, Hungary

^c Research Center for Catalysts and Catalytic Processes, Faculty of Chemistry, University of Bucharest, 4-12, Blv. Regina Elisabeta, 030018 Bucharest, Romania



ARTICLE INFO

Article history:

Received 4 February 2014

Received in revised form 5 October 2014

Accepted 11 October 2014

Keywords:

Esterification

Acetic acid

n-Butanol

n-Butyl acetate

Supported tungsta catalysts

ABSTRACT

The liquid-phase esterification of acetic acid with *n*-butanol has been studied over tungsten oxide supported on alumina, silica and silica-alumina containing two different W loadings. They were prepared by the impregnation of precipitated supports and characterized using X-ray diffraction, N₂ adsorption, SEM-EDX and NH₃-TPD techniques. The effects of esterification conditions including the reaction time and temperature, the acid-to-alcohol mole ratio, the amount of catalyst and the catalyst reusability as well as the effect of reactant pre-adsorption on the reaction conversion were investigated. The best catalytic performance was obtained with WO₃ supported on silica-alumina with a silica-to-alumina mole ratio of 0.4 (10W-Si(0.4)Al sample). The activity of the different catalysts ranged as follows (the conversion of acetic acid at 120 min reaction time in parenthesis): 10W-Si(0.4)Al (95.5) > 10W-Al (86.2) > 10W-Si(1.0)Al (82.1) > 10W-Si(2.5)Al (79.8) > 5W-Al (77.5) > 10W-Si (75.9) > 5W-Si (70.6). The catalytic activity correlated well with the total number of acid sites determined by NH₃-TPD. In all cases the reaction was completely selective to *n*-butyl acetate. Reactant pre-adsorption experiments suggested that the reaction follows the Langmuir-Hinshelwood mechanism. A good reusability of the 10W-Si(0.4)Al catalyst after three reaction cycles was observed.

© 2014 Elsevier B.V. All rights reserved.

1. Introduction

The oxides of elements with valence five or higher present strong to very strong Brønsted acidity [1] which make them good candidates as solid acid catalysts. Indeed, in the last decade, a high number of studies showed that tungsta [2–9], molybdena [10–12], vanadia [13,14] and niobia [15] supported on appropriate supports were effective catalysts for the esterification reaction, one of the fundamental acid-catalyzed reactions.

Concerning the esterification reaction of acetic acid with *n*-butanol, this is the most viable route for producing butyl acetate which is an important chemical being used in large quantities as a solvent in the lacquer industry and coating manufacture, extractant and dehydrator [16–18]. It is also able to replace the toxic

and teratogenic ethoxy ethyl acetate, often used as a solvent [19]. Nb₂O₅/SiO₂–Al₂O₃ has been studied as catalyst for this reaction showing conversions as high as 87% with 100% selectivity for butyl acetate (8 h reaction time at 120 °C) [15]. MoO₃/Al₂O₃ and V₂O₅/Al₂O₃ were shown to be able to catalyze the esterification reaction of acetic acid with *n*-butanol showing conversions of 81 and 63%, respectively, and 100% selectivity for *n*-butyl acetate at 100 °C and 2 h reaction time [11,14]. Improved catalytic performances of the V₂O₅/Al₂O₃ catalyst can be obtained by adding MoO₃ [13].

Because of their high acidity, the supported WO₃ catalysts showed very good catalytic performances in different esterification reactions but, to the best of our knowledge, they were not studied as catalysts for the esterification of acetic acid with *n*-butanol.

The main objective of this research work was to obtain suitable catalysts for the liquid phase esterification process. Supported WO₃ on γ-alumina, silica and silica-alumina were prepared by impregnation and characterized by XRD, nitrogen adsorption, SEM-EDX and NH₃-TPD. Their catalytic properties for the esterification of acetic acid with *n*-butanol were investigated in details.

* Corresponding author at: Laboratory of Chemical Technology and Catalysis, Department of Organic Chemistry, Biochemistry & Catalysis, Faculty of Chemistry, University of Bucharest, 4-12, Blv. Regina Elisabeta, 030018 Bucharest, Romania. Tel.: +40 213051464; fax: +40 213159249.

E-mail addresses: ioancezar.marcu@chimie.unibuc.ro, ioancezar.marcu@yahoo.com (I.-C. Marcu).

2. Experimental

2.1. Catalysts preparation

Al_2O_3 support was prepared from $\text{Al}(\text{NO}_3)_3 \cdot 9\text{H}_2\text{O}$ (Fluka Analytical) by precipitation with ammonium carbonate (Lachema) at controlled pH of 6.5. SiO_2 support was prepared from $\text{Na}_2\text{SiO}_3 \cdot 5\text{H}_2\text{O}$ (Sigma-Aldrich) by precipitation with ammonium chloride (Lach-Ner) at controlled pH of 6.5. $\text{SiO}_2\text{-Al}_2\text{O}_3$ supports with three different $\text{SiO}_2/\text{Al}_2\text{O}_3$ mol ratios, i.e. 0.4, 1.0 and 2.5, labeled Si(0.4)Al, Si(1.0)Al and Si(2.5)Al, respectively, were prepared by coprecipitation using $\text{Al}(\text{NO}_3)_3 \cdot 9\text{H}_2\text{O}$ and Na_2SiO_3 as precursors. Ammonium chloride was used as precipitating agent at controlled pH of 6.5 when both Al and Si ions were completely coprecipitated. All the precipitates were separated by filtration and washed with distilled water, dried in air at 100 °C for 12 h and, finally, calcined at 600 °C for 4 h. WO_3 was introduced at two concentrations, 5 and 10% by weight, via incipient wetness impregnation of supports with aqueous ammonium tungstate (Schering-Kahlbaum) solutions containing appropriate amounts of tungsten. After impregnation, the samples were dried in air at 100 °C for 12 h and then calcined at 600 °C for 4 h. The 5 wt% WO_3 /support and 10 wt% WO_3 /support samples were labeled 5W-Al, 5W-Si, 10W-Al, 10W-Si, 10W-Si(0.4)Al, 10W-Si(1.0)Al and 10W-Si(2.5)Al, where Al and Si stand for Al_2O_3 and SiO_2 , respectively.

2.2. Catalysts characterization

The crystalline phases were investigated by the X-ray diffraction (XRD) method. XRD patterns were obtained with a Philips PW 3710 type diffractometer equipped with a Cu K_α source ($\lambda = 1.54\text{\AA}$), operating at 50 kV and 40 mA. They were recorded over the 5–70° angular range with 0.02° (2 θ) steps and an acquisition time of 1 s per point. Data collection and evaluation were performed with PC-APD 3.6 and PC-Identify 1.0 software.

The surface areas of the catalysts were measured from the adsorption isotherms of nitrogen at –196 °C using the BET method with a Micromeritics ASAP 2020 sorptometer. The samples were first out-gassed at 300 °C for 4 h in the degas port of the adsorption apparatus. The pore size distribution curves were calculated using the desorption branch of the isotherms with the Barrett-Joyner-Halenda (BJH) method.

Qualitative and quantitative electron probe microanalyses were performed using a Philips XL 30 ESEM (Environmental Scanning Electron Microscope) having EDX (Energy Dispersive X-ray) analyzer. An accelerating voltage of 20 kV was used. The powder samples were fixed on a holder and sample compartment was evacuated in order to prevent the electrical charging. Electron beams were very finely focused. Therefore, elemental analysis of very small area on specimen surface was done in so-called spot mode. In this case, the diameter of the microprobe beam was about 0.5 μm which can penetrate volume of the surface layer at about 5 μm^3 . The spot mode analysis was carried out for three points of the same sample. Simultaneously, the surface of the sample was photographed, the micrographs obtained being presented in Fig. S1.

The acidity of the catalysts was estimated by temperature-programmed desorption of ammonia (NH_3 -TPD). About 0.1 g of the catalyst sample was dehydrated at 500 °C in dry air for 1 h and purged with N_2 for 0.5 h. The sample was then cooled down to 100 °C under the flow of N_2 , and NH_3 was supplied to the sample until its saturation. For desorption of the physisorbed ammonia, a nitrogen stream was passed over the sample, at the same temperature, until no more NH_3 was observed in the exit flow. Finally, the chemisorbed NH_3 was desorbed in a N_2 flow by increasing the temperature successively up to 350 °C and 500 °C with a heating rate of

10 °C/min. The ammonia desorbed was bubbled through a solution of sulfuric acid. The acid in excess was titrated with a solution of NaOH, the amount of ammonia desorbed being then calculated. The ammonia desorbed at temperatures lower than 350 °C accounted for the weak and medium-strength acid sites while that desorbed in the temperature range from 350 to 500 °C, for the strong acid sites.

2.3. Catalytic test

The esterification reactions of acetic acid (Chimactiv, 99.5%) with *n*-butanol (Riedel-de Haën, 99.5%) were performed in a 150 mL two-neck flask equipped with a condenser and an additional port for sample withdrawal. The above assembly was heated using a thermostated hotplate. The reaction was carried out at 100 °C with a molar quantity of acetic acid of 0.09 and an *n*-butanol-to-acetic acid molar ratio varied from 1 to 3. Cyclohexane (Riedel-de Haën, 99.5%) was always added to the reaction mixture for water removal, the cyclohexane-to-acetic acid molar ratio being kept at 1. The amount of catalyst was varied between 0.5 and 1.3% of the mass of mixture charge in the reaction. All the experiments were conducted at a speed of agitation of 600 rpm to avoid diffusional limitations as reported elsewhere [11,14]. All the catalysts used in the reaction were in the powder form. Pre-adsorption experiments were performed by premixing the catalyst with one of the reactants or both at room temperature for 24 h followed by heating to 100 °C and charging the preheated remaining reactant. Samples from the organic layer were withdrawn at regular intervals and analyzed with a Thermo Finnigan chromatograph using a DB-5 column and a flame ionization detector. Under the employed conditions of reaction butyl acetate was the only product detected. The mass balances, calculated after a reaction time of 120 min, were always higher than 95%.

3. Results and discussion

3.1. Characterization of the catalysts

The XRD patterns of supported WO_3 on alumina and silica-alumina (Fig. 1) showed only broad lines corresponding to γ -alumina (PDF 10-425) and, in addition for silica-alumina-supported samples, a halo between 15 and 35° (2 θ) due to amorphous silica. No signal of WO_3 crystals on alumina and silica-alumina supports was observed suggesting that either the dispersion of WO_3 on the support was high or the WO_3 crystallite size was very small. On the other hand, lines corresponding to both monoclinic (PDF 83-950) and hexagonal (PDF 33-1387) WO_3 crystals were present on silica support in addition to the very broad peak between 15 and 35° (2 θ).

The textural properties of the catalysts are summarized in Table 1. It can be observed that the specific surface areas were relatively high due to the dispersion effect of porous carrier and ranged from 184 to 377 $\text{m}^2\text{ g}^{-1}$. Both the surface area and the pore volume depended on the nature of support and WO_3 loading. Thus, the surface areas and pore volumes of alumina-supported samples were lower than those of silica-supported ones while, as expected, they had intermediate values for the silica-alumina-supported samples. At the same time, the surface areas and pore volumes of the samples with lower WO_3 loading were higher compared to the samples with higher WO_3 loading. All the catalysts displayed typical type IV nitrogen adsorption/desorption isotherms (according to IUPAC classification) with a clear hysteresis loop characteristic of mesoporous materials with cylindrical pores [20], as showed in Fig. 2. The catalysts displayed well-defined pore size distributions (Fig. S2), the average pore diameters being presented in Table 1. The pore size distributions have been obtained from the desorption branch

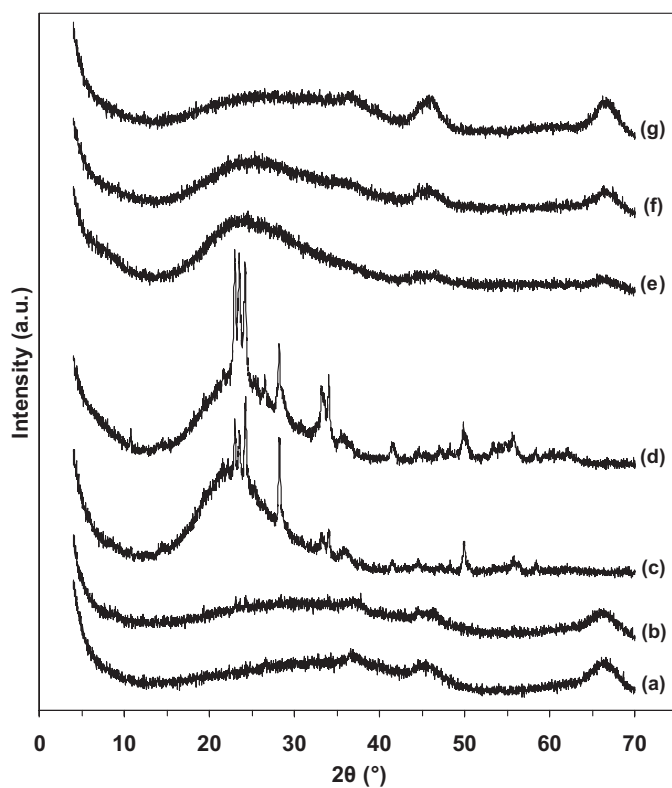


Fig. 1. X-ray diffraction patterns of the WO_3 catalysts supported on alumina, silica and silica-alumina: (a) 5W-Al, (b) 10W-Al, (c) 5W-Si, (d) 10W-Si, (e) 10W-Si(2.5)Al, (f) 10W-Si(1.0)Al, and (g) 10W-Si(0.4)Al.

of N_2 isotherms. Except for 10W-Si(2.5)Al sample, all the catalysts show narrow pore size distributions in the mesopore range, i.e. from 2 to 10 nm. The silica-supported samples have bimodal pores with maxima at about 3.8 and 4.8 nm. For the 10W-Si(2.5)Al sample a broader peak was detected with a maximum at 5.5 nm and a shoulder at 9.9 nm.

The chemical compositions of the catalysts, determined by EDX analysis, are reported in Table 1. They showed that the tungsten content was higher than the nominal value for all the samples. This is not surprising taking into consideration that EDX analysis give, in the conditions used, the surface and subsurface rather than bulk composition of the solids. On the other hand, it can be observed that for the silica-alumina-supported samples, the silica-to-alumina ratios were close to the nominal values.

The tungsten surface densities, expressed as the number of W atoms per nanometer square area (W-atoms nm^{-2}) were calculated using the following equation [4]:

$$\text{Surface density} = \frac{[(\% \text{wt. } \text{WO}_3 / 100) \times 6.023 \times 10^{23}]}{[M_{\text{WO}_3} \times \text{SSA} \times 10^{18}]}$$

Table 1
Textural properties, chemical composition and W surface density of supported WO_3 catalysts.

Catalyst	Surface area ($\text{m}^2 \text{g}^{-1}$)	Pore volume ($\text{cm}^3 \text{g}^{-1}$)	Average pore diameter ^a (nm)	WO_3 (wt%)	$\text{SiO}_2/\text{Al}_2\text{O}_3$ mol ratio	W surface density (W-atoms nm^{-2})
5W-Al	204	0.262	4.2	11.2	–	1.43
10W-Al	184	0.245	4.2	17.1	–	2.41
5W-Si	377	0.487	3.7 and 4.9	7.0	–	0.48
10W-Si	359	0.434	3.8 and 4.7	18.4	–	1.34
10W-Si(0.4)Al	193	0.259	3.7	14.0	0.43	1.89
10W-Si(1.0)Al	209	0.354	5.5	15.2	0.97	1.89
10W-Si(2.5)Al	249	0.433	5.5 and 9.9	16.6	2.60	1.73

^a Maxima of pore size distribution.

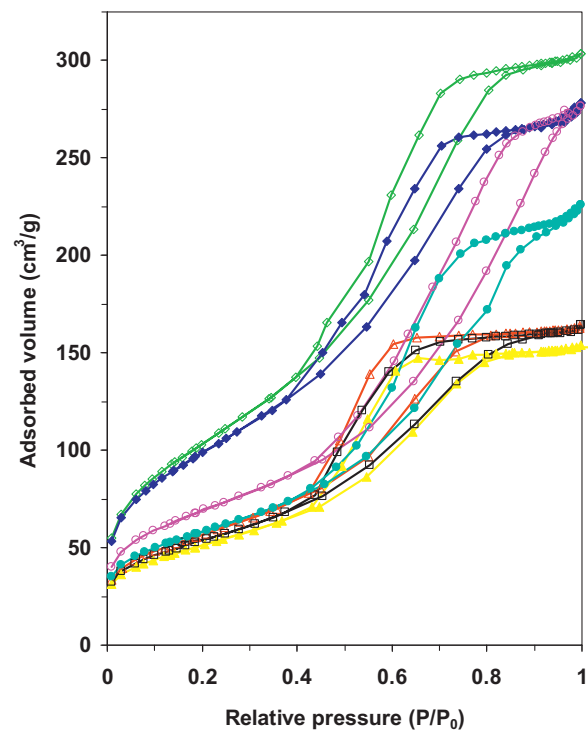


Fig. 2. Nitrogen adsorption/desorption isotherms of the supported WO_3 catalysts: 5W-Al (▲), 10W-Al (△), 5W-Si (◇), 10W-Si (◆), 10W-Si(2.5)Al (○), 10W-Si(1.0)Al (●), 10W-Si(0.4)Al (□).

where M_{WO_3} is the formula weight of WO_3 and SSA, the specific surface area in $\text{m}^2 \text{g}^{-1}$. They are presented in Table 1.

An important factor determining the reactivity of the catalysts used in the esterification reaction is the acidity. The total acidities of the catalysts, expressed as the total number of acid sites per gram of catalyst, have been determined by NH_3 -TPD and are presented in Table 2.

It can be observed that both the total acidity and the number of strong acid sites follow the order: 10W-Si(0.4)Al > 10W-Al > 10W-Si(1.0)Al > 10W-Si(2.5)Al > 5W-Al > 10W-Si > 5W-Si. The total number of acid sites per unit surface roughly follows the same order. As the WO_3 loading increases on alumina and silica supports the acidity value increases. For the alumina-silica-supported catalysts, the total amount of acid sites increased with decreasing $\text{SiO}_2/\text{Al}_2\text{O}_3$ ratio suggesting that alumina has a certain contribution to the total acidity. The total acidity expressed as the total number of acid sites per unit surface of catalyst increases with increasing the tungsten surface density, as shown in Fig. 3. This correlation suggests that the acidity of the supported WO_3 catalysts is mainly due to the surface tungsten. However, it can be observed in Fig. 3 that for 10W-Si(0.4)Al catalyst the contribution of the support to the total acidity is significant.

Table 2

Number and strength of acid sites of the catalysts.

Catalysts	Number of acid sites (mmol/g)		Total number (mmol/g)	10^3 (mmol/m ²)
	Weak and medium	Strong		
5W-Al	0.32	0.22	0.54	2.65
10W-Al	0.31	0.38	0.69	3.75
5W-Si	0.27	0.19	0.46	1.22
10W-Si	0.31	0.21	0.52	1.45
10W-Si(0.4)Al	0.40	0.41	0.81	3.88
10W-Si(1.0)Al	0.39	0.25	0.64	3.32
10W-Si(2.5)Al	0.34	0.23	0.57	2.29

3.2. Esterification of acetic acid with *n*-butanol

The effects of esterification conditions including the reaction time and temperature, the acid-to-alcohol molar ratio, the amount of catalyst and the catalyst reusability as well as the effect of reactant pre-adsorption on the reaction conversion were investigated, the results obtained being presented below.

3.2.1. Influence of reaction time

The influence of the reaction time was studied in the following reaction conditions: *n*-butanol-to-acetic acid mole ratio 3:1, the catalyst representing 0.7 wt% of the mass of mixture charge in the reaction and the reaction temperature being kept at 100 °C. In these conditions, the selectivity of *n*-butyl acetate being, in all cases, 100%, the conversion of acetic acid can represent the yield of *n*-butyl acetate. The results obtained are shown in Fig. 4 and indicate that the catalytic performance of the WO₃ supported on silica–alumina and alumina is better than that supported on silica. Also, the conversion of acetic acid was higher for the catalysts with higher WO₃ loading.

The activity of the different catalysts at 120 min reaction time ranged as follows (the conversion of acetic acid in parenthesis): 10W-Si(0.4)Al (95.5) > 10W-Al (86.2) > 10W-Si(1.0)Al (82.1) > 10W-Si(2.5)Al (79.8) > 5W-Al (77.5) > 10W-Si (75.9) > 5W-Si (70.6). This order is similar to that corresponding to the total number of acid sites determined by ammonia chemisorption. Moreover, linear correlations between the total acidity of the catalysts

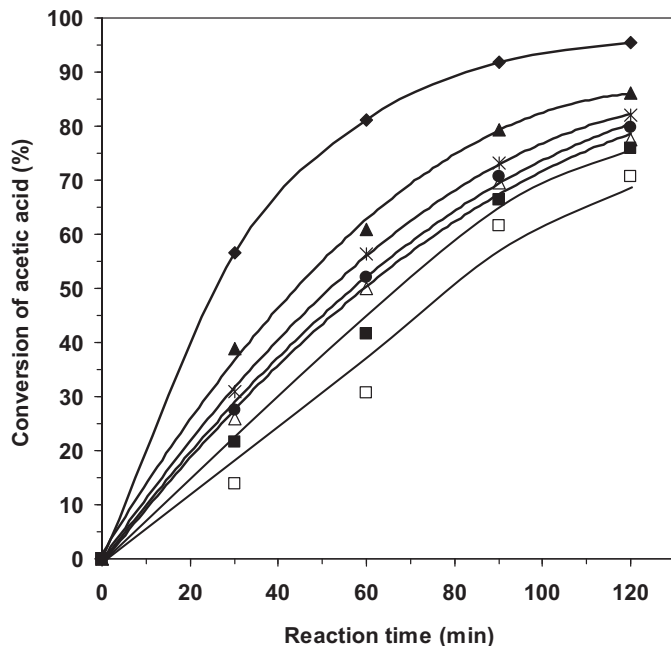


Fig. 4. Conversion of acetic acid as a function of the reaction time on the different catalysts: 5W-Si (□), 10W-Si (■), 5W-Al (△), 10W-Al (▲), 10W-Si(2.5)Al (●), 10W-Si(1.0)Al (*), 10W-Si(0.4)Al (◆). Reaction conditions: *n*-butanol-to-acetic acid mole ratio 3:1, 0.7 wt% catalyst and reaction temperature 100 °C.

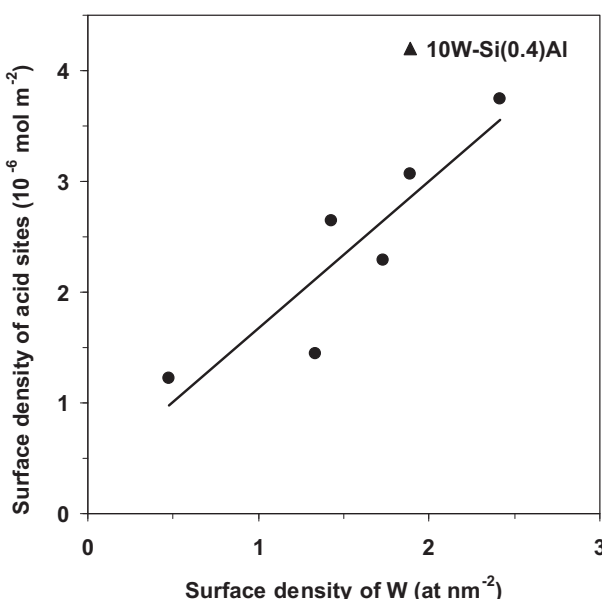


Fig. 3. Variation of the total intrinsic acidity of the catalysts as a function of their tungsten surface density.

and both the turnover frequencies (TOF) and conversions calculated for 30 min reaction were observed, as shown in Fig. 5. It is noteworthy that the conversions of the best supported WO₃ catalysts in this series were higher than those of other systems in the literature over the same amount of time [21–24], including commercially available solid acid catalysts [25].

3.2.2. Influence of reaction temperature

The influence of reaction temperature on the esterification of acetic acid with *n*-butanol over 10W-Si(0.4)Al catalyst was evaluated by varying the reaction temperature from 90 to 110 °C at a *n*-butanol-to-acetic acid mole ratio of 2:1 for 120 min with 0.7 wt% catalyst. The results obtained are shown in Fig. 6. It can be seen that the conversion of acetic acid increased substantially with the increase in reaction temperature indicating that the reaction is controlled by chemical steps. Note that the selectivity remained 100%. The values of the turnover frequency (TOF) calculated for 30 min of reaction are 503.9, 568.7 and 648.2 mol [mol H⁺]⁻¹ h⁻¹ at 90, 100 and 110 °C, respectively. The apparent activation energy calculated from the slope of the Arrhenius plot $\ln(\text{TOF}) = f(1/T)$ presented in Fig. S3 was found to be 14.5 kJ mol⁻¹. This value is quite similar to those reported for the esterification of acetic acid with *n*-butanol over other solid acid catalysts [26].

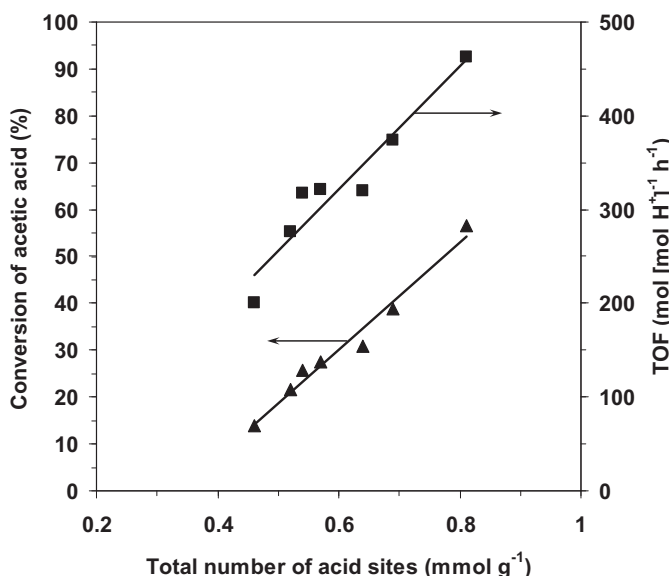


Fig. 5. Variation of the turnover frequency (TOF) and conversion calculated for 30 min reaction as a function of the total acidity of the catalysts. Reaction conditions: *n*-butanol-to-acetic acid mole ratio 3:1, 0.7 wt% catalyst and reaction temperature 100 °C.

3.2.3. Influence of reactant molar ratio

To shift the equilibrium in the sense of ester formation, an excess of alcohol is usually used [27,28]. Thus, the initial acid-to-alcohol molar ratio was varied from 1:1 to 1:3 for the reaction performed over all the supported WO₃ catalysts at 100 °C with 0.7 wt% catalyst. The results obtained after 120 min reaction time are shown in Fig. 7. It can be observed that, as expected, for all the catalysts studied the conversion substantially increased by increasing the initial acid-to-alcohol mole ratio from 1:1 to 1:3.

3.2.4. Influence of catalyst amount

The amount of the catalyst was varied from 0.5 to 1.3% by mass of the total reaction mixture using 10W-Si(0.4)Al, 10W-Si(1.0)Al

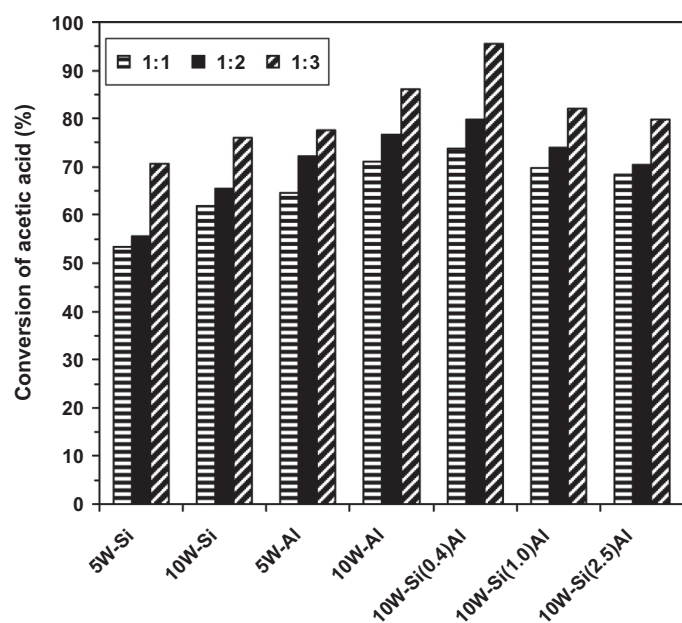


Fig. 7. Effect of acid-to-alcohol mole ratio on the esterification of acetic acid with *n*-butanol over supported WO₃ catalysts. Reaction conditions: temperature 100 °C, 0.7 wt% catalyst and reaction time 120 min.

and 10W-Al as catalysts, while keeping the *n*-butanol-to-acetic acid mole ratio at 3:1, the reaction temperature at 100 °C and the reaction time at 90 min (Fig. 8). In all cases, the conversion of acetic acid increased almost linearly with increasing the catalyst amount from 0.5 to ca. 1% and then it tends to a plateau. This suggests that 1 wt% is the optimal mass fraction of the catalyst in the reaction medium.

3.2.5. Reusability of the catalyst

Reusability of solid acid catalysts is very important in viewpoint of practical application. The 10W-Si(0.4)Al catalyst was used for recycling experiments carried out under the following reaction conditions: acetic acid-to-*n*-butanol mole ratio was 1:3, 0.7 wt% catalyst, reaction temperature 100 °C and 2 h reaction time. After 2 h of reaction the catalyst was separated by filtration, washed with distilled water several times, dried at 120 °C in air and then used

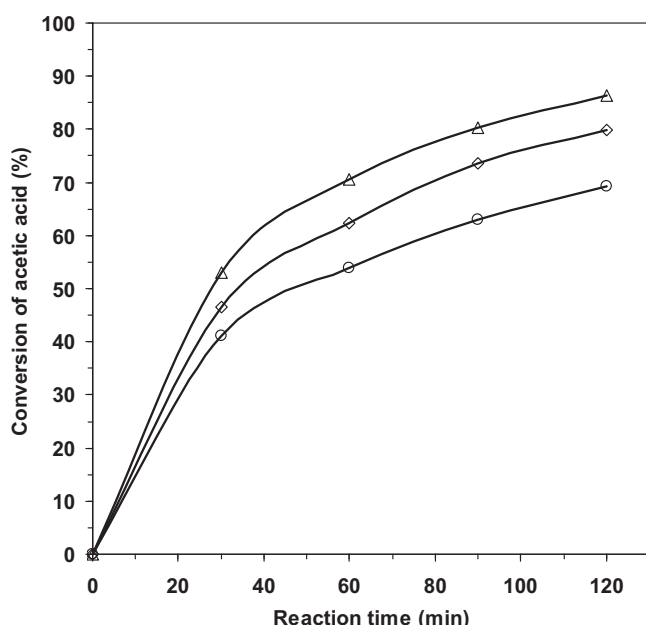


Fig. 6. Conversion of acetic acid as a function of the reaction temperature for 10W-Si(0.4)Al catalyst (○ – 90 °C; ◇ – 100 °C and △ – 110 °C). Reaction conditions: *n*-butanol-to-acetic acid mole ratio 2:1, 0.7 wt% catalyst.

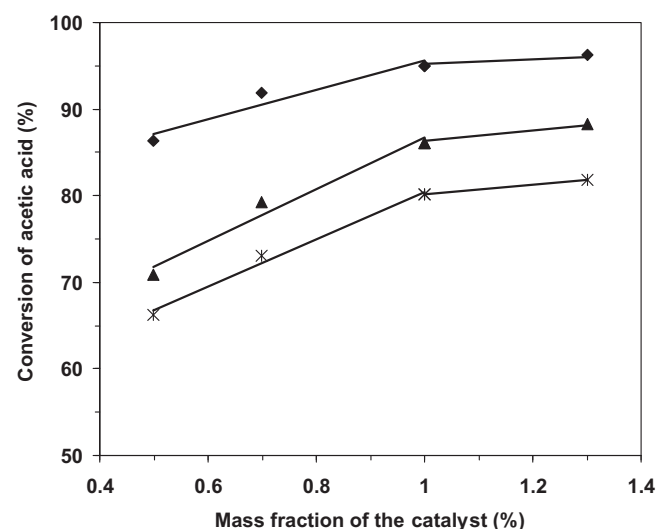


Fig. 8. Effect of catalyst concentration on the esterification of acetic acid with *n*-butanol using 10W-Si(0.4)Al (◆), 10W-Si(1.0)Al (▲) and 10W-Al (*) as catalysts. Reaction conditions: temperature 100 °C, acetic acid-to-*n*-butanol molar ratio = 1:3 and reaction time 90 min.

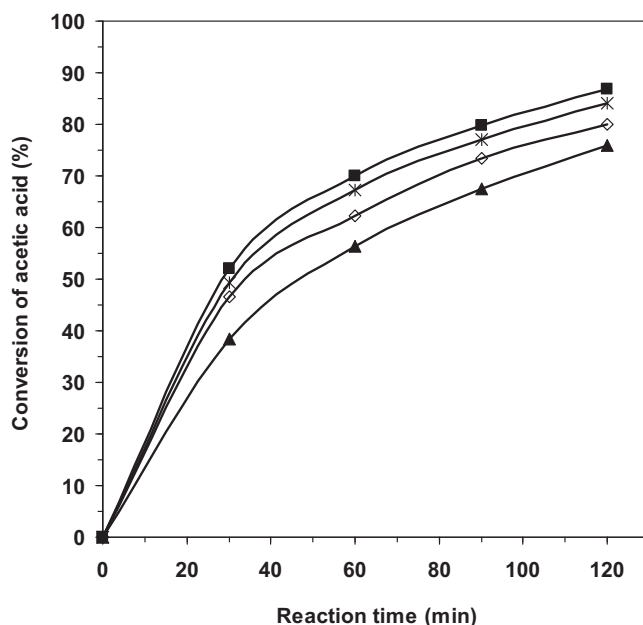


Fig. 9. The effect of reactant pre-adsorption on the 10W-Si(0.4)Al catalyst with a *n*-butanol-to-acetic acid mole ratio of 1:2, 0.7 wt% catalyst and reaction temperature 100 °C: (◊) no pre-adsorption; (■) pre-adsorption of acetic acid; (▲) pre-adsorption of *n*-butanol; (*) pre-adsorption of both acetic acid and *n*-butanol.

in the esterification reaction with a fresh reaction mixture. The conversion values of 95.5, 96.2 and 95.1% observed for three successive reaction cycles suggest a good reusability of the 10W-Si(0.4)Al catalyst in the esterification of acetic acid with *n*-butanol.

3.2.6. Effect of reactant pre-adsorption

An important mechanistic question in esterification reactions catalyzed by solid acids is the involvement of one or two surface-bounded species corresponding to Eley–Rideal or Langmuir–Hinshelwood type mechanism, respectively. Alkbay and Altiookka [29], Teo and Saha [30] and Lee et al. [31] determined that two surface adsorbates were involved in the rate-determining step of liquid-phase esterification of acetic acid with isoamyl alcohol using a cation-exchange resin as catalyst. Miao and Shanks [32] also proposed a mechanism with the kinetically relevant step involving reaction of two surface adsorbates for liquid-phase esterification of acetic acid with methanol over propylsulfonic acid-functionalized SBA-15 catalyst. At the same time, Altiookka and Çitak [33] proposed that esterification reactions of acetic acid with isobutanol catalyzed by cation-exchange resin occur via a single-site Eley–Rideal pathway in which an adsorbed alcohol molecule reacts with an acid molecule from the bulk phase. An Eley–Rideal type mechanism was also proposed for the esterification of acetic acid with *n*-butanol catalyzed by zirconia-supported silicotungstic acid [34] and for the esterification of acetic acid with methanol catalyzed by silica-supported Nafion [35]. Information about the mechanism involved can be obtained by pre-adsorption of alcohol, acid or both alcohol and acid on the solid catalyst before the esterification [13,32]. Thus, the effect of reactant pre-adsorption has been studied with the 10W-Si(0.4)Al catalyst for a *n*-butanol-to-acetic acid mole ratio of 2:1 and with 0.7 wt% catalyst. It has been premixed with acetic acid, *n*-butanol or both acetic acid and *n*-butanol for 24 h at room temperature and then heated until reaching the reaction temperature, i.e. 100 °C. At this moment the preheated remaining reactant was added. The obtained conversion versus time curves are shown in Fig. 9 where the curve corresponding to the reaction without premixing of reactants is also presented for comparison.

It can be observed that the highest conversion values were obtained when premixing the catalyst with acetic acid and decreased following the order: premixing with acetic acid > premixing with both acetic acid and *n*-butanol > no premixing > premixing with *n*-butanol. As the reaction rate was higher when premixing the catalyst with both acetic acid and *n*-butanol compared with the reaction with no premixing this suggests that the reaction needs the chemisorption of both acetic acid and *n*-butanol involving a Langmuir–Hinshelwood type mechanism. The results in Fig. 9 also suggested a strong adsorption of *n*-butanol and a weak adsorption of acetic acid competing for the same adsorption sites. This is in line with other literature results proposing a stronger chemisorption of the alcohol than the acid [30,36].

4. Conclusion

WO₃ supported on γ-alumina, silica and silica-alumina were found to be active and stable solid acid catalysts for the esterification of acetic acid with *n*-butanol. The catalytic activity was a function of the total acidity of the solid which was associated to its surface tungsten. It ranged as follows (the conversion of acetic acid at 120 min reaction time in parenthesis): 10W-Si(0.4)Al (95.5) > 10W-Al (86.2) > 10W-Si(1.0)Al (82.1) > 10W-Si(2.5)Al (79.8) > 5W-Al (77.5) > 10W-Si (75.9) > 5W-Si (70.6). In all the esterification reactions the selectivity for *n*-butyl acetate was 100%. The optimal mass fraction of the catalyst in the reaction medium was found to be around 1 wt%. The catalytic properties of the 10W-Si(0.4)Al catalyst are maintained after three successive reactions. Reactant pre-adsorption experiments suggested that the reaction follows the Langmuir–Hinshelwood mechanism with a much stronger adsorption of *n*-butanol than acetic acid.

Acknowledgments

The authors are grateful to Dr. Éva Makó, Oravetz Dezső and Dr. Jozsef Kovacs from the University of Pannonia for their expert technical assistance with the analytical measurements.

Appendix A. Supplementary data

Supplementary data associated with this article can be found, in the online version, at <http://dx.doi.org/10.1016/j.molcata.2014.10.014>.

References

- [1] G. Busca, in: J.L.G. Fierro (Ed.), *Metal Oxides: Chemistry and Applications*, CRC Press, Boca Raton, 2006 (chapter 9).
- [2] C. Baroi, S. Mahto, C. Niu, A.K. Dalai, *Appl. Catal. A* 469 (2014) 18–32.
- [3] M.N. Alaya, M.A. Rabah, *J. Alloys Compd.* 575 (2013) 285–291.
- [4] A.A. Costa, P.R.S. Braga, J.L. de Macedo, J.A. Dias, S.C.L. Dias, *Microporous Mesoporous Mater.* 147 (2012) 142–148.
- [5] Y.-M. Park, S.-H. Chung, H.J. Eom, J.-S. Lee, K.-Y. Lee, *Bioresour. Technol.* 101 (2010) 6589–6593.
- [6] I. Jiménez-Morales, J. Santamaría-González, P. Maireles-Torres, A. Jiménez-López, *Appl. Catal. A* 379 (2010) 61–68.
- [7] P. Wongmaneebil, B. Jongsomjit, P. Praserthdam, *Catal. Commun.* 10 (2009) 1079–1084.
- [8] D.E. López, K. Suwannakarn, D.A. Bruce, J.G. Goodwin Jr., *J. Catal.* 247 (2007) 43–50.
- [9] S. Ramu, N. Lingaiah, B.L.A. Prabhavathi Devi, R.B.N. Prasad, I. Suryanarayana, P.S. Sai Prasad, *Appl. Catal. A* 276 (2004) 163–168.
- [10] A. Bail, V.C. dos Santos, M.R. de Freitas, L.P. Ramos, W.H. Schreiner, G.P. Ricci, K.J. Ciuffi, S. Nakagaki, *Appl. Catal. B* 130–131 (2013) 314–324.
- [11] G. Mitran, E. Makó, Á. Rédey, I.C. Marcu, *Catal. Lett.* 140 (2010) 32–37.
- [12] R. Wan, S.-C. Li, Y.-P. Yuan, T.-Y. Li, C.-H. Du, *Modern Chem. Ind.* 30 (Suppl. 1) (2010) 37–41.
- [13] G. Mitran, O.D. Pavel, I.C. Marcu, *J. Mol. Catal. A* 370 (2013) 104–110.
- [14] G. Mitran, É. Makó, Á. Rédey, I.C. Marcu, *C. R. Chim.* 15 (2012) 793–798.

- [15] V.S. Braga, I.C.L. Barros, F.A.C. Garcia, S.C.L. Dias, J.A. Dias, *Catal. Today* 133–135 (2008) 106–112.
- [16] Kirk-Othmer, *Encyclopedia of Chemical Technology*, vol. 9, fourth ed., John Wiley & Sons, New York, 1994, pp. 797.
- [17] G.B. Varadwaj, K.M. Parida, *Catal. Lett.* 141 (2011) 1476–1483.
- [18] S. Blagov, S. Parada, O. Bailer, P. Moritz, D. Lam, R. Weinand, H. Hasse, *Chem. Eng. Sci.* 61 (2006) 753–765.
- [19] S. Steinigeweg, J. Gmehling, *Ind. Eng. Chem. Res.* 41 (2002) 5483–5490.
- [20] K.S.W. Sing, D.H. Everett, R.A.W. Haul, L. Moscou, R.A. Pierotti, J. Rouquerol, T. Siemieniewska, *Pure Appl. Chem.* 57 (1985) 603–619.
- [21] P. Sharma, S. Vyas, A. Patel, *J. Mol. Catal. A* 214 (2004) 281–286.
- [22] Y. Wang, Y. Gan, R. Whiting, G. Lu, *J. Solid State Chem.* 182 (2009) 2530–2534.
- [23] K.M. Parida, G.C. Behera, *Catal. Lett.* 140 (2010) 197–204.
- [24] B. Li, W. Ma, J. Liu, S. Zuo, X. Li, *J. Colloid Interface Sci.* 362 (2011) 42–49.
- [25] T.A. Peters, N. Benes, A. Holmen, J. Keurentjes, *Appl. Catal. A* 297 (2006) 182–188.
- [26] J.H. Sepúlveda, J.C. Yori, C.R. Vera, *Appl. Catal. A* 288 (2005) 18–24.
- [27] J. Lilja, J. Wärnå, T. Salmi, L. Pettersson, J. Ahlkvist, H. Grénman, M. Rönnholm, D.Yu. Murzin, *Chem. Eur. J.* 115 (2005) 1–12.
- [28] G.D. Yadav, M.B. Thathagar, *React. Funct. Polym.* 52 (2002) 99–110.
- [29] E.Ö. Akbay, M.R. Altiokka, *Appl. Catal. A* 396 (2011) 14–19.
- [30] H.T.R. Teo, B. Saha, *J. Catal.* 228 (2004) 174–182.
- [31] M.J. Lee, H.T. Wu, H.M. Lin, *Ind. Eng. Chem. Res.* 39 (2000) 4094–4099.
- [32] S. Miao, B.H. Shanks, *J. Catal.* 279 (2011) 136–143.
- [33] M.R. Altiokka, A. Çitak, *Appl. Catal. A* 239 (2003) 141–148.
- [34] K.M. Parida, S. Mallick, *J. Mol. Catal. A* 275 (2007) 77–83.
- [35] Y.J. Liu, E. Lotero, J.G. Goodwin, *J. Catal.* 242 (2006) 278–286.
- [36] M.T. Sanz, R. Murga, S. Beltran, J.L. Cabezas, J. Coca, *Ind. Eng. Chem. Res.* 41 (2002) 512–517.